communications earth & environment

Article

https://doi.org/10.1038/s43247-024-01252-7

Thermogenic methane and hydrogen generation in subducted sediments of the Nankai Trough

Check for updates

Noriyuki Suzuki [1] ✉, Koutaro Koike[1,3], Jun Kameda [1,4] & Gaku Kimura[2]

Active and widespread CH_4 accumulations and emissions in the Nankai Trough subduction zone are attested by numerous mud volcanoes, gas plumes, and gas hydrates containing biogenic and thermogenic CH_4. However, the source rocks of the thermogenic CH_4 and the geological source of H_2 for microbial CH_4 production by methanogens remain uncertain. Here, we reveal the timing and rate of thermogenic CH_4 and H_2 generation from shales and metapelites associated with oceanic plate subduction in the Nankai Trough by gas and geochemical analyses. The results show that the thermogenic CH_4 and H_2 are generated mainly in the underthrust sediments below the décollement. The sustainable H_2 supply from the underthrust sediments can potentially contribute to microbial CH_4 production. The findings enhance our understanding of the active CH_4 emission, large-scale gas hydrate formation, and subseafloor biosphere in the oceanic plate subduction zone.

Methane (CH_4) is an energy resource and a greenhouse gas. Its accumulation in the subsurface and emission on the seafloor have long drawn research attention. On the other hand, the source and supply of hydrogen (H_2) in the geosphere have also attracted growing interest because H_2 supply is a critical factor for sustaining the deep biosphere and the production of microbial CH_4. In the geosphere, molecular H_2 is produced from the degradation of sedimentary organic matter by H-producing bacteria[1], inorganically by hydrothermal alteration such as serpentinization[2,3], and mechanochemically by the interaction between water and silicate rock fracturing[4,5]. H_2 is also generated thermally with aromatization, condensation, and graphitization of sedimentary organic matter[6–8]. In an arc-trench system, marine sediments on the oceanic plate are transported deep into the crust and undergo metamorphic processes. The underthrust sediments below the detachment thrust (décollement) of an oceanic plate in an arc-trench system may serve as CH_4 and H_2 source rocks and play an essential role in the accumulation and emission of CH_4 in the plate subduction zone. However, few studies have addressed these potential roles of the underthrust sediments so far.

The Nankai Trough subduction zone in southwest Japan is a typical example of the arc-trench system composed of inner and outer prisms covered by forearc sediments and the underthrust sediments subducting with the Philippine Sea plate[9,10] (Fig. 1). The CH_4 accumulations and emissions, such as mud volcanoes, methane plumes, and gas hydrates or bottom simulating reflectors (BSRs), occur widely in the forearc basin and accretionary prism of the Nankai Trough[11–14] (Fig. 1). The total amount of CH_4 in gas hydrate-bearing sediments in the eastern Nankai Trough has been estimated to be about 40 trillion cubic feet ($1.1 \times 10^{12} m^3$), probably one of the world's largest marine gas hydrate deposits[15]. Dissolved-in-water type gas deposits (dissolved gas deposits), composed mainly of CH_4, are distributed in the coastal land of Tokai and southwestern Kyushu near the Nankai Trough, and CH_4 seeps also occur in these areas[16–20]. These CH_4 accumulations and emissions are thermogenic and/or microbial[13,16–24]. It is, however, unclear where and how much thermogenic CH_4 is generated in the Nankai Trough subduction zone. In addition, although the active CH_4 production by methanogens in the organic-poor environment requires abiogenic geological H_2, the origin and source of geological H_2 remain uncertain[1]. Understanding the spatial distribution and rate of CH_4 and H_2 generation in the subduction zone will clarify the geological context of active CH_4 accumulations and emissions in an arc-trench system. In this regard, we focused on the underthrust sediments below the décollement of the subducting oceanic plate.

In contrast to the considerable time required to form conventional oil and gas deposits, gas hydrates and mud volcanoes are formed within a geologically short time in regions where the CH_4 flux is high. The convergence rate of the Philippine Sea Plates with the southwest Japan Arc is about 50–60 mm yr^{-1} (year)[10,25–27], a much faster rate than the subsidence

[1]Department of Earth and Planetary Sciences, Hokkaido University, Kita-ku, N10 W8, Sapporo 060-0810, Japan. [2]Yokohama Institute for Earth Sciences, Japan Agency for Marine-Earth Science and Technology (JAMSTEC), 3173-25, Showa-machi, Kanazawa-ku, Yokohama-city, Kanagawa 236-0001, Japan. [3]Present address: Toho Zinc Co., Ltd., Tekko Building, 1-8-2 Marunouchi, Chiyoda-ku, Tokyo 100-8207, Japan. [4]Present address: Institute for Planetary Materials, Okayama University, 827 Yamada, Misasa, Tottori 682-0193, Japan. ✉e-mail: suzu@sci.hokudai.ac.jp

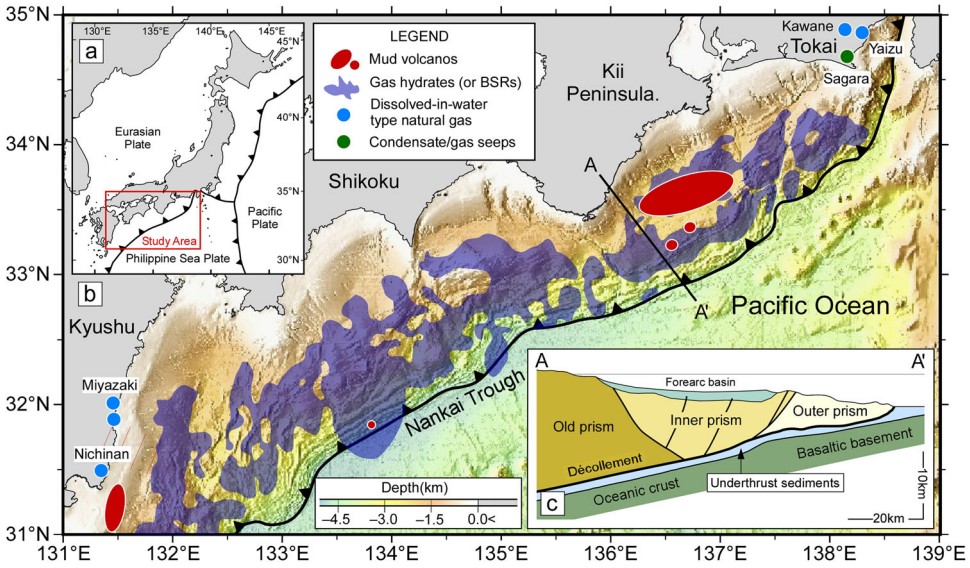

Fig. 1 | Methane accumulations and emissions in the Nankai Trough subduction zone. **a** Location of the study area. **b** Distribution of mud volcanoes[14], gas hydrates (BSRs)[12], dissolved gas deposits[16,18,20], and condensate/gas seeps[17,18] in the Nankai Trough subduction zone. **c** Schematic geological section of the Nankai Trough off the Kii Peninsula[10]. The black line with triangles represents the trough axis of the Nankai Trough. The water-depth map is courtesy of the Hydrographic and Oceanographic Department of the Japan Coast Guard.

rate of the sedimentary basin. The subsidence rate is related to the heating rate, which can affect the thermal decomposition rate of sedimentary organic matter. The maturity level of the thermogenic CH_4 and H_2 generation in the subduction zone can be estimated based on residual gases in shales and metapelites from subaerial accretionary prisms. From the heating and subsidence rates of the accretionary prisms and the underthrust sediments, we have predicted the spatial distributions and rates of thermogenic CH_4 and H_2 generation in the Nankai Trough subduction zone. The expulsion and migration of thermogenic CH_4 and H_2 have been discussed, considering the active seismogenesis and their solubility in the deep fluids. The present study shows that the generation rate of thermogenic CH_4 in the underthrusut sediments is much higher than in the accretionary prisms, and the thermogenic CH_4 in the Nankai Trough subduction zone is mainly derived from the underthrust sediments. Following the thermogenic CH_4 generation, the thermogenic H_2 is generated in the underthrust sediments during the metagenesis to metamorphism in the deep subduction zone. The thermogenic H_2 derived from the underthrust sediments can be another potential geological source of H_2 for microbial CH_4 production in the Nankai Trough. The sustainable supply of thermogenic CH_4 and H_2 from the underthrust sediments associated with the oceanic plate subduction can contribute to the accumulation and emission of CH_4 represented by the formation of large-scale gas hydrates in the Nankai Trough.

Results and discussion

Organic matter in the underthrust sediments

The oceanic lithosphere ages of the subducting Philippine Sea Plate slab in southwest Japan are estimated to be 15–30 Myr[28]. Underthrust sediments consist of pelagic sediments that have been transported by the movement of the oceanic plate and marine and terrestrial sediments deposited in the trench. The pelagic sediments of the Philippine Sea Plate are composed of claystone, radiolarian and diatomaceous siliceous mudstones, and nannofossil calcareous mudstones[29,30]. Rock-Eval® analyses for the Ocean Drilling Program (ODP)/Deep-Sea Drilling Project (DSDP)/Integrated Ocean Drilling Program (IODP) sediment samples equivalent to the subducting section in the Nankai Trough showed that the Cretaceous to Quaternary sediments deposited far from the continents were richer in marine organic matter (Type II kerogen)[30]. Conversely, those deposited in the ocean-continent subduction zone showed higher terrestrial organic matter content (Type III kerogen). Frequent earthquakes in the subduction zone trigger the remobilization of surficial sediments along the landward slope of the trough, resulting in marine and terrestrial sediment accumulation[31,32]. In the Nankai Trough, the sediment sections on the Philippine Sea Plate are relatively thick (more than 1000 m), and the upper and younger parts of sedimentary layers were accreted landward to form the accretionary prism with plate subduction[9,10]. The underthrust sediments subducted beneath the accretionary prism are the lower and older sedimentary sections, for which information is lacking since few drilling operations have penetrated through all the sedimentary layers above the basaltic basement.

The total organic carbon (TOC) concentrations of Neogene sediments from IODP Expedition 333 drill sites (C0011 and C0012) close to the Nankai Trough are low, ranging from 0.2 to 0.5 wt%[33]. Based on the results of ocean drilling programs (ODP, DSDP, and IODP) in the Pacific Ocean, the average TOC concentration of the underthrust sediments of the Philippine Sea Plate is 0.5 wt%[30]. Although this TOC concentration may be somewhat higher than the average TOC concentrations of shale (0.44 wt%, $n = 28$) and metapelites (0.33 wt%, $n = 41$) from the old accretionary prisms in the Shikoku region (Supplementary Table 1), a TOC of 0.5 wt% is reasonable when considering thermal decomposition during diagenesis to metamorphism. The present study assumes an initial TOC concentration of 0.5 wt% to estimate the thermogenic CH_4 and H_2 generation in the accretionary prism and underthrust sediments of the Nankai Trough.

Heating rate in the accretionary prism and underthrust sediments

Since the difference in the heating rate of accretionary prisms and underthrust sediments directly affects the generation rate of thermogenic CH_4 and H_2, the difference in their heating rates in the subduction zone was first examined. The heating rate of sediments in the Nankai Trough subduction zone can be estimated based on the thermal structure, movement of the accretionary prism, and the convergence rate of the Philippine Sea Plate. The Kumano-nada region, offshore of the Kii Peninsula, is one of the sections in the Nankai Trough where the subduction history of the Philippine Sea Plate, the formation of accretionary prism, and thermal structure, respectively, have been well investigated[9,10] (Fig. 2). In the subduction zone 25–100 km landward from the trough axis, the heat flow is nearly constant at 50–65 mW m^{-2} [34,35]. The depth-temperature relationship below 200 °C in the Kumano-nada basin is obtained from the long-term borehole monitoring system installed at Site C0002 during the IODP Expedition 332[36], extrapolated to the subsurface temperature distribution in the Kumano-nada region (Fig. 2 and Supplementary Fig. 1). Isotherms above 200 °C (Fig. 2) were from the modeling results of the thermal structure around the Philippine Sea Plate (Supplementary Figs. 2, 3)[37,38].

The active subduction of the Philippine Sea Plate with formations of the forearc basin and new accretionary prism began about 6.0 Myr ago[9,10]. The subduction zone in its present configuration was formed about 2.2 Myr ago[39,40]. Based on sediment accretion models in the Nankai Trough[41,42], we estimated the lateral velocity of the accretionary prism. The thickness of the

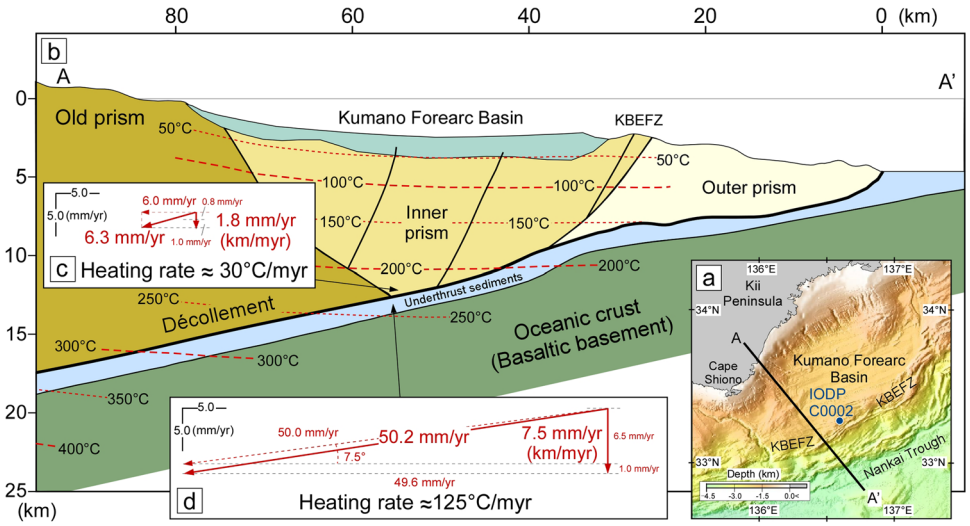

Fig. 2 | Subsurface isotherms and annual subduction and heating rates of sediments in the Nankai Trough subduction zone. **a** Location of the geological section with IODP Site C0002[36]. **b** Subsurface isotherms superimposed on the schematic geological section of the Kumano-nada region off the Kii Peninsula. The boundary between the outer and the inner prisms is the Kumano basin edge fault zone (KBEFZ)[76]. **c** The annual subduction and heating rates of the inner accretionary prism. **d** The annual subduction and heating rates of the underthrust sediments. The water-depth map is courtesy of the Hydrographic and Oceanographic Department of the Japan Coast Guard.

accretionary prism in the Kumano-nada region gradually increases landward. Considering the total volume of the outer prism and its initiation 2.2 Myr ago, the average annual volume of sediment accretion for one km length of the trough is estimated at approximately 53.2×10^3 m^3 yr^{-1} km^{-1} (Supplementary Figs. 4, 5). The lateral velocity of the accretionary prism gradually decreases with increased thickness and distance from the trough. At its thickest, the current lateral velocity of the prism is approximately 6.0 mm yr^{-1} (Supplementary Fig. 5). The vertical subsidence rate of the accretionary prism can be estimated from the burial rate of the Kumano forearc basin (about 1.0 mm yr^{-1}) and the taper angle (7.5°) of the subducting plate. The average subduction rate of the Philippine Sea Plate along the Nankai Trough was set at 50 mm yr^{-1} [25,27,43]. As a result, the movement velocities of the deepest part of the inner prism and the underthrust sediments were estimated at approximately 6.3 mm yr^{-1} and 50.2 mm yr^{-1}, respectively (Fig. 2 and Supplementary Fig. 5). The heating rates of sedimentary rocks are mainly related to the vertical velocity of movement and the temperature gradient. Considering the subsurface temperature distribution in the Kumano-nada region, the heating rates of the accretionary prism and the underthrust sediments are estimated to be approximately 30 °C Myr^{-1} and 125 °C Myr^{-1}, respectively (Fig. 2).

Timing of thermogenic CH_4 and H_2 generation in the subduction zone

The thermogenic CH_4 and H_2 generation in the subduction zone was predicted based on the concentration changes of residual gases in shales and metapelites with increasing diagenetic and metamorphic temperatures. Although the residual gas concentration in pelitic rocks has an upper limit because of the limited capacity to retain gaseous components, the relative residual gas concentration depends roughly on the total gas composition generated during diagenesis and metamorphism. Shales and metapelites were resampled from the same sampling site of the old accretionary prism[8] (Supplementary Fig. 6) and analyzed for residual gas using an improved analytical method. A small peak of O_2 relative to the N_2 peak in the chromatogram shows negligible air contamination during analysis (Supplementary Fig. 7). The CH_4, C_2H_6 (ethane), CO_2, N_2, and H_2 were detected in shales and metapelites from the old accretionary prism (Supplementary Table 1). The relationship between vitrinite reflectance (VR) and the maximum heating temperature of the samples was determined using Easy%RoV[44], assuming the heating rate of 30 °C Myr^{-1}, the heating rate for the inner accretionary prism in the Nankai Trough subduction zone (Fig. 2).

The concentration changes of residual C_2H_6, CH_4, and H_2 with increasing diagenetic and metamorphic temperatures are shown in Fig. 3, with some typical gas chromatograms of residual gas. Residual C_2H_6 attains peak concentration at around VR = 2.0% and almost disappears at the maturity level of VR = 2.5%. The residual CH_4 concentration rises at about 130° to 150 °C (VR = 0.7%) and reaches a peak (1500–1700 μL g TOC^{-1}) at about 220° to 230 °C (VR = 2.5%), after which it decreases probably due to the formation of graphitic carbonaceous material[45,46]. The residual H_2 concentration rises at around 150° to 200 °C (VR = 1.0–2.0%) and shows a higher concentration in the pelitic rocks at metagenesis to metamorphism (VR > 4.0%). In metapelites that experienced higher temperatures of more than 300 °C, the volume concentration of H_2 exceeds that of CH_4 (Fig. 3). The residual CO_2 concentration decreases drastically from several hundred to less than 10 μL g TOC^{-1} at VR < 2.0 % (Supplementary Table 1), possibly due to the decarboxylation of sedimentary organic matter and expulsion of CO_2 with porosity reduction. Since some CO_2 is adsorbed on the mineral surface during pulverization, the residual CO_2 concentration measured is less than the total CO_2 retained in shale rocks[8]. The concentration of residual N_2 ranges mostly from 100 to 1000 μL g TOC^{-1} and does not show any systematic change with increasing temperature (Supplementary Table 1). The origin of residual N_2 is currently unknown. The residual C_2H_6, CH_4, and H_2 in the shales and metapelites are mainly derived from the thermal decomposition of sedimentary organic matter[8].

Thermogenic CH_4 is mainly generated by the thermal cracking of hydrocarbons and kerogen during the thermal condensation of macromolecular intermediates and kerogen. Therefore, the amount of thermogenic CH_4 generation is related to the expulsion of hydrocarbons. In the case of accretionary prisms and underthrust sediments, the average TOC concentration is estimated to be so low (0.5 wt%) compared to ordinary petroleum source rocks, suggesting minimal expulsion of hydrocarbons because of their poor saturation in the pore space. Hence, from the viewpoint of thermal decomposition, thermogenic CH_4 generation is regarded as proceeding almost in a closed system. In closed-system pyrolysis experiments of sedimentary organic matter, thermogenic CH_4 concentration gradually increases with increasing thermal maturation from VR = 0.7–4.0%, and C_2H_6 disappears at around VR = 2.5%[47,48], a pattern consistent with the relationships between maturation stages (VR values) and residual CH_4 and C_2H_6 concentration changes in the old accretionary prism (Fig. 3). The maturation level of the oil generation zone is generally variable due to the difference in kerogen type. However, the timing of wet and dry gas generations is not so dependent on the initial kerogen type because mature kerogens are characterized by similar chemical structures dominated by C-C bonds[49]. We assumed the C_2H_6 and CH_4 generation zones were at VR < 2.5% and VR = 1.5 to 4.0%, respectively, considering the closed-system pyrolysis experiments and the change of residual gas concentrations in the old accretionary prism.

Hydrogen atoms and radicals produced during oil and wet gas generation are consumed immediately by secondary reactions, e.g., the

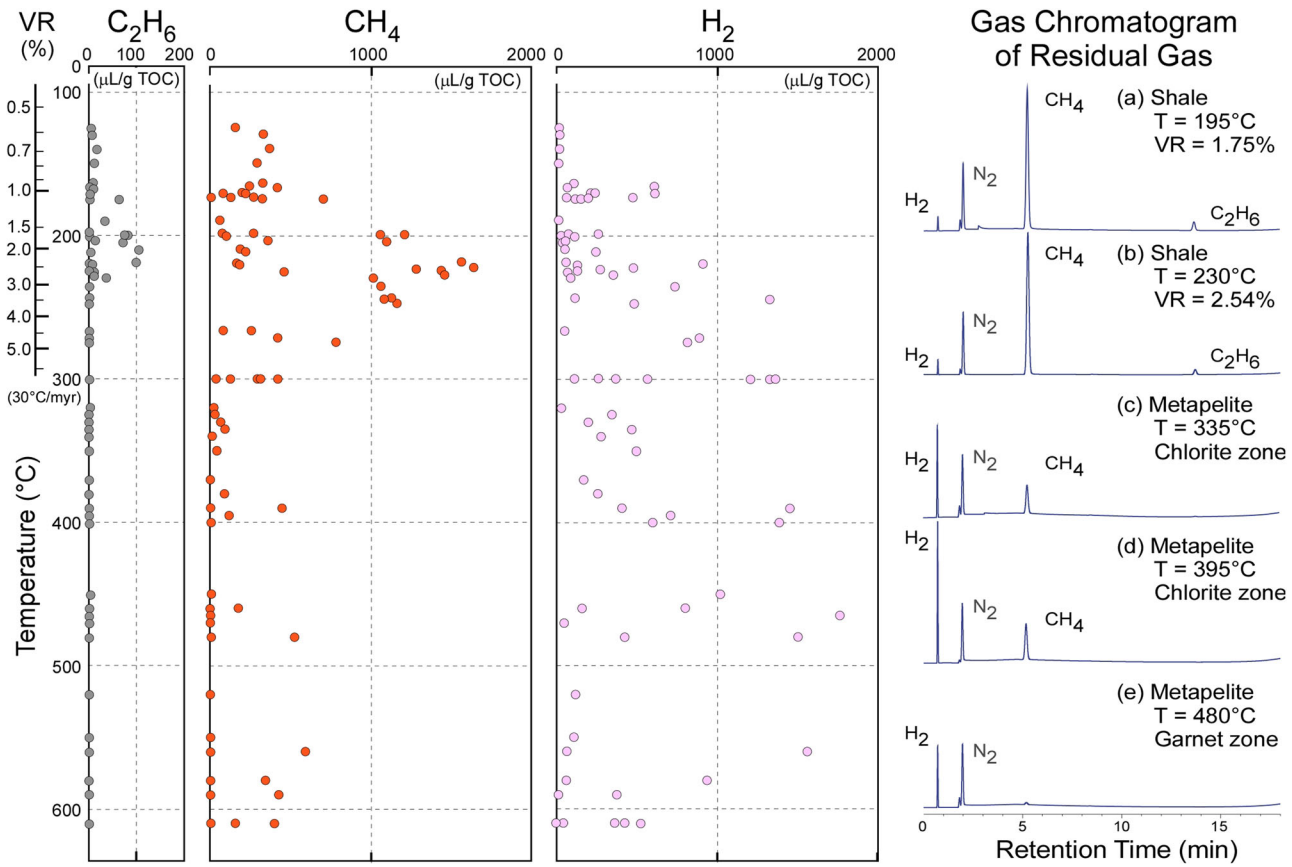

Fig. 3 | Concentration changes with temperature for residual CH_4, C_2H_6, and H_2 in shales and metapelites. The relationship between VR and the maximum paleotemperature was computed using Easy%RoV[44], assuming a heating rate of 30 °C Myr^{-1}. Maximum temperatures attained by metapelites were estimated from metamorphic mineral assemblages. Some typical gas chromatograms for the residual gases show changes in the relative abundances of H_2, N_2, CH_4, and C_2H_6 with increasing the maximum temperature. A part of the dataset is from Suzuki et al.[8].

hydrogenation of alkenes[7]. The formation of molecular H_2 proceeds during the carbonization and graphitization of carbonaceous material in the metagenetic and metamorphic stages. The generation of thermogenic H_2 from kerogen at a high temperature, following CH_4 generation, has been confirmed in laboratory pyrolysis experiments[6,7]. We assumed that the thermogenic H_2 generation zone starts from VR = 2.5%, corresponding to the maturity level of wet gas disappearance. The progress of the organic reaction under high pressure is generally retarded compared to that under low pressure[50,51]. Since metamorphism in the Nankai Trough proceeds under relatively higher pressures than other subduction zones[52], the timing of thermogenic H_2 generation may be retarded compared to the old accretionary prism. In the present study, the thermogenic CH_4 and H_2 generation zones have been estimated to range from VR = 1.5 to 4.5% and VR > 2.5%, respectively. Temperatures in the inner accretionary prism and the underthrust sediments corresponding to these VR values are different because of different heating rates. According to the Easy%RoV, the VR values of 1.5%, 2.5%, and 4.5% for the inner accretionary prism with a lower heating rate of 30 °C Myr^{-1} correspond to 194°, 222°, and 268 °C, respectively. On the other hand, the same VR values for the underthrust sediments with a higher heating rate of 125 °C Myr^{-1} are equivalent to 204°, 233°, and 279 °C, respectively, which are about 10 °C higher than in the inner accretionary prism. The thermogenic CH_4 and H_2 generation zones in the Nankai Trough subduction zone are shown in a schematic geological section of the Kumano-nada region off the Kii Peninsula (Fig. 4).

Generation rate of thermogenic CH_4 and H_2 in the subduction zone

To clarify the respective contribution of the underthrust sediments and accretionary prisms to the thermogenic CH_4 generation in the subduction zone, their annual CH_4 generation rates were estimated and compared. Although the sediments in the subduction zone contain some terrestrial organic matter, we assumed the same Type II (marine) kerogen and TOC concentration (0.5 wt%) for comparison convenience. According to pyrolysis experiments of kerogen in a closed system, the ultimate yield of CH_4 from Type II kerogen was approximately 300 mg CH_4 g TOC^{-1} [47,48]. Therefore, the annual generation rate of CH_4 can be estimated from the TOC concentration, the apparent sediment density (2.6 g cm^{-3}), and the movement velocity of the underthrust sediments and the inner prism. The underthrust sediments of about one km thick are moving through the CH_4 generation zone at a subduction rate of about 50.2 mm yr^{-1} in the Kumano-nada region (Fig. 2). Under these conditions, the annual generation rate of CH_4 in the underthrust sediments subducting along one km length of the Nankai Trough was estimated to be approximately 2.7×10^5 m^3 yr^{-1} km^{-1}. In the case of the accretionary prism, only the sediments at the deepest part of the inner prism are within the CH_4 generation zone (Fig. 4). The old accretionary prism acts as a static backstop and comprises highly mature sediments and metamorphic, volcanic, and plutonic rocks[10,43], suggesting a low thermogenic CH_4 and H_2 generation.

In the inner prism, it can be assumed that about two km thick sediment layer above the décollement is moving landward through the CH_4 generation zone at a rate of 6.3 mm yr^{-1} (Fig. 4). Like the underthrust sediments if the ultimate amount of thermogenic CH_4 was generated within the two km thick sediment layer moving at 6.3 mm yr^{-1}, the annual CH_4 generation rate in the accretionary prism along one km length of the Nankai Trough is estimated at approximately 6.9×10^4 m^3 yr^{-1} km^{-1}. However, the highest temperature of the CH_4 generation zone in the inner prism is about 225 °C (VR = 2.5%), and only a limited part has intersected the CH_4 generation zone. Since the area of the inner prism in the CH_4 generation zone is less

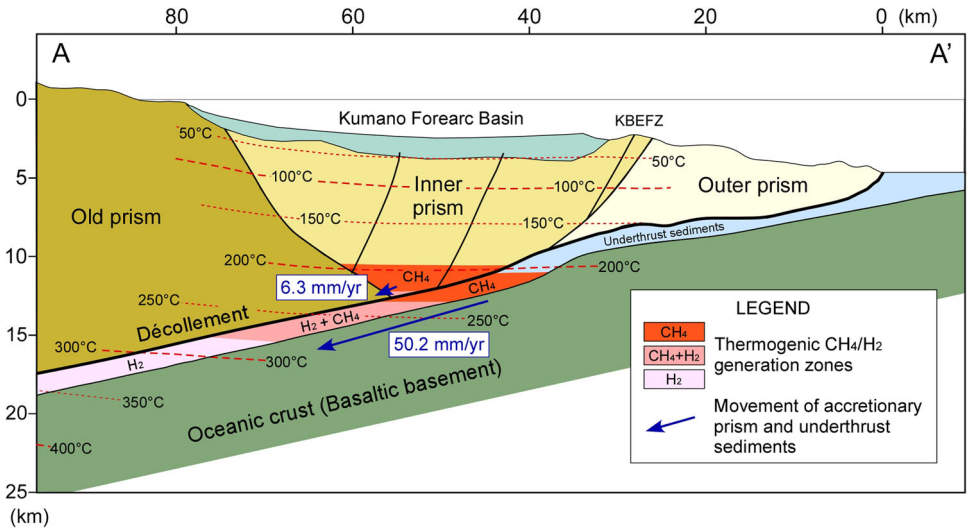

Fig. 4 | Thermogenic CH_4 and H_2 generation zones in the Nankai Trough subduction zone. The thermogenic CH_4 and H_2 generation zones within the accretionary prism and underthrust sediments are indicated in the schematic geological section of the Kumano-nada region off the Kii Peninsula. Temperatures in the deepest part of the inner prism are not high enough to generate $CH_4 + H_2$. The subducting underthrust sediments pass through the $CH_4 + H_2$ generation zone and sustainably generate CH_4 and H_2.

than half of the whole thermogenic CH_4 generation zone (ca. 195–270 °C), the generation level of thermogenic CH_4 in the inner prism is less than 50 % of the ultimate level. Therefore, the annual generation rate of CH_4 in the inner prism along one km of the Nankai Trough is estimated to be less than 3.5×10^4 m^3 yr^{-1} km^{-1}, much lower than the underthrust sediments. The higher generation rate of thermogenic CH_4 in the underthrust sediments is attributed to sufficient thermal maturation and a faster subduction rate. The volumetric concentration of residual H_2 in highly mature shales and metapelites is similar to residual CH_4, suggesting that the thermogenic H_2 generation rate is comparable to that of thermogenic CH_4 (Fig. 3). Thermogenic CH_4 and H_2 are being generated in the underthrust sediments for at least the past 2.2 Myr, according to the evolutionary history of the subduction of the Philippine Sea Plate[9,10,39,40,43]. The total thermogenic CH_4 generation during the last 2.2 Myr reaches approximately 5.9×10^{11} m^3 per one km length of the Nankai Trough. The movement velocity of the inner prism indicates that its deepest part arrived at the CH_4 generation zone about 2.0 Myr ago. Since then, continued thermogenic CH_4 generation in the inner prism has gradually increased over time. However, the inner prism of the Nankai Trough has not yet reached the thermogenic H_2 generation zone.

Spatial distribution of thermogenic CH_4 and H_2 generation zone

The spatial distribution of the thermogenic CH_4 and H_2 generation zones of the underthrust sediments and the accumulation and emission of CH_4 in the Nankai Trough is shown in Fig. 5. The heating rate of the underthrust sediments is assumed to be the same as the Kumano-nada region at 125 °C Myr^{-1}. Therefore, the CH_4 and H_2 generation zones in Fig. 5 were set at about 205° to 280 °C and >235 °C, respectively. Gas hydrates and BSRs are located away from the thermogenic CH_4 and H_2 generation zones and distributed widely trough-ward. In contrast, mud volcanoes in the Kumano-nada region off the Kii Peninsula and the Hyuga-nada off Nichinan tend to be distributed landward and overlap with the CH_4 and H_2 generation zones (Fig. 5). The $\delta^{13}C$ values of CH_4 from mud volcanoes in the Kumano-nada region from −20 to −40‰[23,24] suggest much contribution of thermogenic CH_4. The dissolved gas deposits are distributed in the coastal area from Miyazaki to Nichinan in the southeastern Kyushu region and Yaizu and Kawane in the Tokai region (Fig. 5). The $\delta^{13}C$ value of CH_4 from dissolved gas deposits and gas seeps in the southeastern Kyushu and the Tokai region ranges from –68‰ to –37‰ and –34‰ to –33‰, respectively[16–20]. Those from Nichinan and the Tokai region near the thermogenic CH_4 generation zone tend to have higher $\delta^{13}C$ values[16–18], suggesting a contribution of thermogenic CH_4. The mud volcanoes and dissolved gas deposits comprising thermogenic CH_4 are located above or near the thermogenic CH_4 generation zone in the underthrust sediments, suggesting a causal relationship. The $\delta^{13}C$ value of CH_4 from gas hydrates in the subduction zone of the Nankai Trough varies from –70‰ to –40‰, and like water-dissolved gas deposits, those near the CH_4 generation zone tend to have higher $\delta^{13}C$ values[22–24]. The BSRs widely distributed in the Nankai Trough are probably indicative of gas hydrates[12,15]. Gas hydrate samples, however, have only been recovered from a limited number of BSRs. Widely distributed gas hydrates possibly contain mainly microbial CH_4, considering the lower $\delta^{13}C$ values of CH_4 in available gas hydrates[13,22].

Expulsion and migration of thermogenic CH_4 and H_2

The thermogenic CH_4 and H_2 generated in the underthrust sediments may cause overpressure in and around the décollement of the subducting plate, as suggested by Raimbourg et al.[30]. The present earthquake rupture area at a depth of 10–20 km along the décollement[10,53,54] almost corresponds to the thermogenic CH_4 and H_2 generation zones in the underthrust sediments (Fig. 4). The expulsion of thermogenic gas from the source rocks presumably occurs intermittently due to the micro and macro fracturing of rocks and releases the overpressure associated with seismogenesis. The expulsion of thermogenic CH_4 and H_2 most likely occurs mainly in their generation zone corresponding to the earthquake rupture area. Many studies on fluids and fluid inclusions in the accretionary prisms and underthrust sediments show active fluid migration in the Nankai Trough subduction zone[41,55,56]. Slab-dehydrated fluids from the oceanic plate contribute to subaerial hot spring emanations in the subduction zone[57,58] as well as fluids expelled in the Kumano forearc basin and Nankai Trough accretionary prisms[59–61]. In addition to slab-dehydrated fluids, fluids expelled from the underthrust sediments due to porosity reduction and clay/silica mineral dehydration migrate widely in the accretionary prisms through décollement megathrust and splay faults[41,57]. The active deep fluids may dissolve CH_4 and H_2 expelled from the source rocks, thus promoting their secondary migration in the Nankai Trough subduction zone.

Following experiments on the solubility of CH_4 in pure water and salt water over a wide range of temperatures and pressures from 0 to 350 °C and 1 to 260 MPa[62–64], Duan and Mao[65] proposed a thermodynamic model for estimating CH_4 solubility in pure water and salt water from 0 to 300 °C and 1 to 200 Mpa. Zhu et al.[66] extrapolated the solubility of H_2 in pure water and salt water from low temperature (100 °C) and low pressure (50 Mpa) experiments[67,68] to 150 °C and 110 Mpa using the particle interaction theory. This theoretical model allows the prediction of the solubility of H_2 in deep fluids in the subduction zone. The solubility of CH_4 and H_2 in pure water from 0 to 150 °C and 1 to 110 Mpa are shown in Fig. 6. The 110 Mpa nearly corresponds to the overburden pressures at a burial depth of 4.5 km[36,52]. At 60 °C, the solubility of CH_4 and H_2 in pure water generally increases with increasing temperature and pressure (Fig. 6). However, the increase in

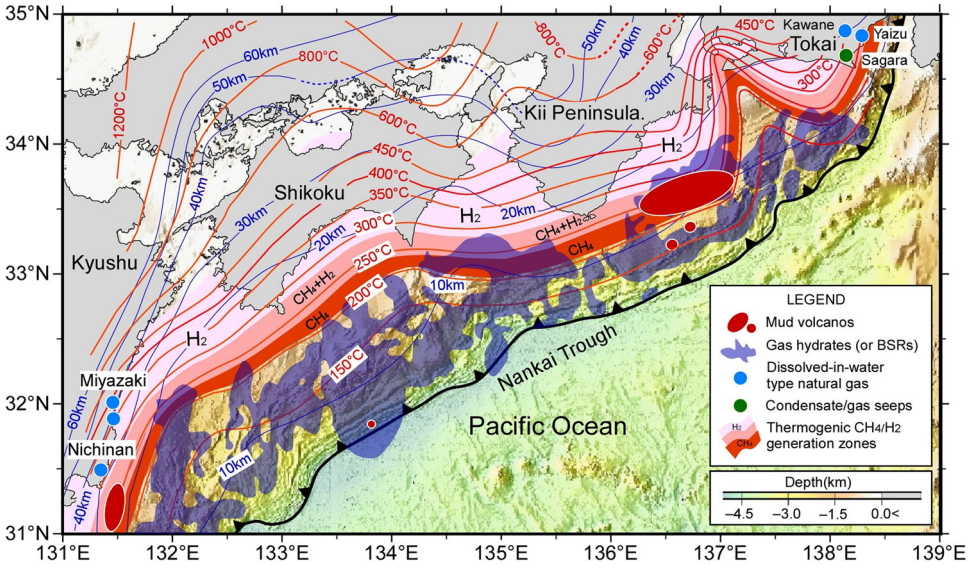

Fig. 5 | The spatial distributions of the thermogenic CH_4 and H_2 generation zones in the Nankai Trough. The red contours show the temperatures of the upper surface of the subducting Philippine Sea Plate in the Kyushu, Shikoku, and Kii Peninsula regions[37] and the Tokai region[38], respectively. The blue contours show the depths of the upper boundary of the Philippine Sea Plate[77–79]. The water-depth map is courtesy of the Hydrographic and Oceanographic Department of the Japan Coast Guard.

solubility of CH_4 with increasing temperature and pressure is not as prominent as that of H_2. Since the thermogenic CH_4 generation from the source rocks (TOC = 0.5 wt%) has been assumed to be 300 mg g TOC^{-1} (1.9×10^{-2} mol g TOC^{-1}), the ultimate generation of thermogenic CH_4 is approximately 9.5×10^{-5} mol g $Rock^{-1}$. The solubility of CH_4 in water at 300 °C and 200 Mpa, roughly corresponding to the thermogenic CH_4 generation zone (10 to 12 km depth), is estimated to be 2.8×10^{-3} mol g H_2O^{-1} [64]. According to the extrapolated porosity curve in the Nankai Trough[36], the sediment porosity at 10 km depth is about 0.75 %. Therefore, in the source rock (density=2.6 g cm^{-3}) with a porosity of 0.75 % at the CH_4 generation zone, approximately 8.1×10^{-6} mol g $Rock^{-1}$ of CH_4 dissolves in water. This is less than 9 % of the ultimate generation of thermogenic CH_4, and much of the thermogenic CH_4 can behave as free gas. Although the TOC concentration of sedimentary rocks in the Nankai Trough is assumed to be much lower than in oil and gas fields, much of the thermogenic CH_4 can still behave as free gas in the deep subduction zone. In oil and gas fields, the main driving force for gas migration from the source rocks to the reservoir is thought to be buoyancy[69], possibly the same for the migration of thermogenic CH_4 and H_2 in the subduction zones. However, because of the smaller radius and higher diffusion rate, molecular H_2 is more widely dispersed than CH_4. Since the solubility of H_2 seems to be higher than CH_4 (Fig. 6), more H_2 than CH_4 possibly migrates as a dissolved species in deep fluids. Although the solubility of H_2 in deep fluids under high pressures and temperatures is not fully clarified, the extrapolated curves in Fig. 6 suggest that more H_2 is dissolved in the deep fluids than CH_4. Understanding the migration of the thermogenic H_2 in the subduction zone is a future research topic.

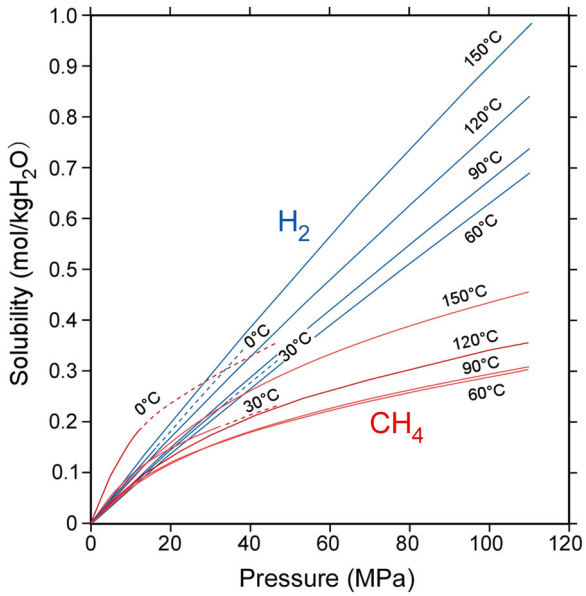

Fig. 6 | Extrapolated solubilities of CH_4 and H_2 in pure water under high temperatures and pressures. The solubilities of CH_4 and H_2 from Duan et al.[64] and Zhu et al.[66], respectively.

Geological sources of H_2 in the Nankai Trough

The generation, expulsion, and possible migration of CH_4 and H_2 in the Nankai Trough subduction zone are summarized in Fig. 7, where accumulation and emission of thermogenic and microbial CH_4 are also shown. The mud volcanoes and dissolved gas deposits are distributed nearly above the thermogenic CH_4 generation zone in the underthrust sediments and accretionary prisms (Fig. 5), suggesting the upward migration of free CH_4 by buoyancy. The formation of mud volcanos occurs intermittently and quickly. It seems unlikely that the eruption of CH_4 to form mud volcanoes occurs by direct CH_4 supply from the deep subduction zone. A type of CH_4 chamber might have developed below the mud volcanoes from which CH_4 is then expelled (Fig. 7). The fracturing and deformation of the CH_4 chamber due to earthquakes and tectonics can induce CH_4 release to form mud volcanoes and CH_4 plumes. In the shallow subsurface, where temperatures are below 60 °C, the solubility of CH_4 in water does not change much with a decrease in temperature and pressure (Fig. 6). Therefore, in an aquifer unsaturated with CH_4 in the shallow subsurface, the free CH_4 migrating upward can be dissolved and trapped by the aquifer to form dissolved gas deposits (Fig. 7).

Several sources of H_2 that might contribute to microbial CH_4 production and sustain the subseafloor biosphere have been proposed. These include H_2 generated by the thermal decomposition of organic matter under relatively low temperatures (<120 °C), H_2 released during hydrothermal rock alteration and serpentinization of oceanic crust, and mechanochemical H_2 generated by the interaction of water with silicate rock fracturing[1]. The open-system pyrolysis of kerogen shows that molecular H_2 is liberated from kerogen by thermal cracking of hetero-bonds, demethylation, aromatization, and condensation[6]. Since the heating rate of the underthrust sediments is higher, the generation rate of such low-temperature thermogenic H_2 is expected to be higher than in the accretionary prisms (Fig. 7). However, hydrous pyrolysis of kerogen under the closed system shows that hydrogen

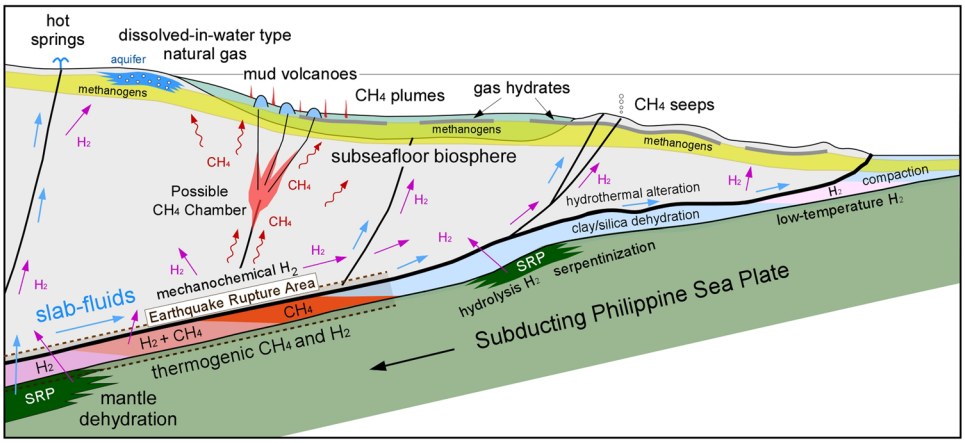

Fig. 7 | The generation, expulsion, and possible migration of CH_4 and H_2 in the Nankai Trough subduction zone. Thermogenic CH_4 and low-temperature H_2 generation zones in the accretionary prism are not indicated. The thermogenic CH_4 and H_2 generation rate in the underthrust sediments below the décollement is higher than in the accretionary prism because of sufficient thermal maturation and a faster subduction rate. The thermogenic CH_4 and H_2 generation zones of underthrust sediments overlap with the earthquake rupture area, suggesting the expulsion of thermogenic CH_4 and H_2 associated with earthquakes. The mud volcanoes and dissolved-in-water type gas deposits with thermogenic CH_4 are distributed nearly above the thermogenic CH_4 generation zones of the underthrust sediments and accretionary prism. Thermogenic CH_4 expelled from the source rocks in the deep subduction zone migrates upward to form mud volcanoes and dissolved gas deposits. Gas hydrates holding biogenic CH_4 are also widely distributed in the Nankai Trough. In organic-poor sedimentary environments, microbial CH_4 production requires abiogenic geological H_2 such as low-temperature H_2 from the thermal decomposition of immature organic matter, hydrolysis H_2 from serpentinization and hydrothermal rock alterations, mechanochemical H_2 from the interaction of silicate rock fracturing and water, and thermogenic H_2 from the thermal alteration of sedimentary organic matter undergoing metagenesis to metamorphism. The migration of the slab dehydrated fluids possibly plays an essential role in transporting H_2 from various sources to the subseafloor biosphere.

radicals generated in the hydrocarbon generation zone are consumed quickly by hydrogen-requiring reactions such as hydrogenation of unsaturated compounds[7]. The hydrocarbon generation in organic-poor sedimentary rocks can be regarded as proceeding in a nearly closed system. Hence, a sufficient amount of molecular H_2 might not be generated in the hydrocarbon generation zone (<120 °C). Seismological analysis has detected slab dehydration and seismic velocity decrease near the surface of the oceanic crust beneath the Shikoku region, suggesting the slab serpentinization by the water released from the slab[70]. Low seismic velocity zones, possibly indicating serpentinization, have also been detected near the surface of the oceanic crust beneath the inner accretionary prism off the Kii Peninsula[71]. The serpentinization of oceanic crust beneath the inner accretionary prisms is thought to be due to the invasion of seawater through the fault system extending to the mantle[72]. The hydrothermal rock alteration and serpentinization, possibly ongoing in the subduction zone, can be a potential source of hydrolysis H_2 (Fig. 7). In the tectonically active subduction zone, the mechanochemical H_2 generated by the interaction of water and silicate rock fracturing can be expected as one of the potential H_2 sources. The active fractures and faults in and around the décollement and earthquake rupture area are likely principal sites of mechanochemical H_2 generation[4,5] (Fig. 7). The thermogenic H_2 generated under relatively high temperatures (>220 °C) discussed in the present study can be another potential geological source contributing to microbial CH_4 production in the subseafloor biosphere (Fig. 7). The expulsion of the thermogenic H_2 from the underthrust sediments is likely to occur associated with seismogenesis. Therefore, the mechanochemical H_2 generated in the earthquake rupture area would behave with the thermogenic H_2 generated in the underthrust sediments.

The H_2 from the sources described above has the potential to contribute to sustaining the subseafloor biosphere and the CH_4 production by hydrogenotrophic methanogens. The low-temperature thermogenic H_2 generated in the shallow sedimentary rocks is comparatively close to the subseafloor biosphere. However, a sufficient amount of low-temperature H_2 generation seems unlikely compared to the thermogenic H_2 generation in the deep subduction zone. Other geological sources of H_2 are located deep in the subduction zone, and long-distance transportation of H_2 is required to support the subseafloor biosphere. The migration of slab-dehydrated fluids is active in the Nankai Trough subduction zone, and such deep fluids may play an essential role in the long-distance transportation of H_2. Compared to gas phase migration, migration of low-solubility gas by solution would be inefficient and require large volumes of fluids. The efficient transport of H_2 by gas phase migration might occur under a limited amount of fluid in the deep subduction zone. However, our knowledge of the solubility and the behavior of H_2 under high pressures and temperatures is currently limited. In addition, the generation rates of H_2 derived from the low-temperature thermal decomposition of organic matter, serpentinization of oceanic crust, and silicate rock fracturing are currently unknown. If the generation rates of H_2 from these geological sources are clarified, comparing them with that of the thermogenic H_2 from the underthrust sediments estimated in this paper, the relative contributions of each source of H_2 for sustaining the subseafloor biosphere will be evident. Moreover, it will deepen our understanding of the geosphere-biosphere interaction leading to the active microbial CH_4 production and the formation of large-scale gas hydrates in the oceanic plate subduction zone.

Methods

Shales and metapelites from old accretionary prisms

Shales and metapelites that experienced a paleo-temperature ranging from 100 to 600 °C were collected from the Shimanto belt and the Sanbagawa metamorphic belt in the Kochi district (Supplementary Fig. 6). Rock samples used in the present study were resampled from the same sampling sites as our previous study[8], and the geological background has been described therein. The Sanbagawa metamorphic belt is divided into the Ooboke and Besshi Nappes based on lithology and metamorphic age. The protoliths of the Sanbagawa metamorphic belt are Triassic to Jurassic and metamorphosed during the Late Cretaceous[73]. The chlorite, garnet, albite-biotite, and oligoclase-biotite metamorphic zones occur along the sampling traverse of the Asemi-gawa River. The metamorphic temperature of metapelites increases gradually from the chlorite zone (300 °C) to the oligoclase-biotite zone (610 °C). The Shimanto belt in the Shikoku region is divided by the Aki Tectonic Line into a northern and a southern belt. The northern belt comprises the Lower Cretaceous Shinjogawa and the Upper Cretaceous Aki groups. The southern belt comprises the Eocene to the Lower Oligocene Muroto Peninsula Group and the Upper Oligocene to the Lower Miocene

Nabae Groups. Shale samples were collected from outcrops of Aki and the Muroto Peninsula Groups distributed along the eastern coast of Tosa Bay. All the shale and metamorphic rocks were deposited in the marine environment with a variable contribution of terrestrial organic matter. There may be some differences in the organic type among the samples, but this would not have much influence on the geochemical characteristics of sedimentary organic matter at the highly mature stage[49]. The paleo-maximum temperature of shales and metapelites was estimated by vitrinite reflectance (VR) and metamorphic mineral assemblages.

Pulverization and residual gas recovery

Residual gas is released from shale fragments during pulverization. Shale fragments were pulverized using a P-6 planetary ball mill and a tungsten carbide mill pot with needle valves for gas transfer lines (Fritsch GmbH, Idar-Oberstein, Germany). The inner volume of the mill pot is 69.6 mL. Fragments of shale and metapelite of 5–7 mm were pulverized in the tungsten carbide mill pot under an ultra-high purity helium (He) atmosphere of 0.3 MPa. Cleaning of the mill pot by ultra-high purity He was repeated three times before the pulverization. Residual gas released in the mill pot was directly transferred to the gas sampling loop of the gas chromatograph through the stainless transfer line. The temperature of the tungsten carbide mill pot during pulverization was below 45 °C. The grain size of the rock powder after the pulverization was measured by a laser diffraction-scattering method using a grain-size analyzer (LA-920: Horiba, Kyoto, Japan) and was generally from 3–7 μm.

Residual gas, elemental analysis, and vitrinite reflectance

The composition of the residual gas in the rock fragments was measured by gas chromatography (GC) using an instrument (7890 A: Agilent, Santa Clara, CA, USA) equipped with a pulsed discharge He ionization detector (PDHID) and a micropacked column containing ShinCarbon-ST 80/100 (2.0 m × 1.0 mm i.d.; Shinwa Co., Nagoya, Japan) (Supplementary Fig. 7). The oven temperature of the GC was programmed to 40 °C for 3 min, increased to 300 °C at a rate of 15 °C min^{-1}, and then held at 300 °C for 15 min. Ultra-high purity He was used as the carrier gas. A constant amount of gas directly transferred from the tungsten carbide mill pot was introduced into the GC column using a 50 μL sampling loop. Compounds were identified and quantified by comparing the retention times with those of reference standards in a gas mixture containing CH_4 (495 ppmv), C_2H_4 (494 ppmv), C_2H_6 (495 ppmv), and CO_2 (480 ppmv) (Taiyo Nippon Sanso Group, Co., Kawasaki, Japan) and the ionization coefficients by Wentworth et al.[74]. The detailed analytical procedure is described in Saito et al.[75]. Total organic carbon (TOC) and total nitrogen (TN) contents were determined using an EA 3000 elemental analyzer (Euro Vector Co., Milan, Italy). The pulverized shale or metapelite was weighed and placed in a silver capsule with drops of 1 N HCl to remove carbonates. The carbonate-free sample was dried at 120 °C for 2 hrs and analyzed by the elemental analyzer. The mean VR of randomly oriented vitrinite grains was measured using a reflection microscope (Eclipse LV100ND; Nikon Corp., Japan) equipped with a stabilized halogen light source and photonic multichannel analyzer (PMA12; Hamamatsu Photonics K. K., Japan). The VR value was measured for a spot diameter of 20 μm at a wavelength of 542.8 nm by comparison with the standard values of polished glasses with VR values of 0.55, 0.79, 1.08, and 1.53%.

Data availability

All data reported in the present study are listed in Supplementary Data, available at https://doi.org/10.6084/m9.figshare.25097237.

Received: 13 September 2023; Accepted: 31 January 2024;
Published online: 21 February 2024

References

1. Parks, P. J. et al. A review of prokaryotic populations and processes in subseafloor sediments, including biosphere: geosphere interactions. *Mar. Geol.* **352**, 409–426 (2014).
2. Seewald, J. S. Organic-inorganic interactions in petroleum-producing sedimentary basins. *Nature* **426**, 327–333 (2003).
3. Mayhew, L. E., Ellison, E. T., McCollom, T. M., Trainor, T. P. & Templeton, A. S. Hydrogen generation from low-temperature water-rock reactions. *Nat. Geosci.* **6**, 478–484 (2013).
4. Kameda, J., Saruwatari, K. & Tanaka, H. H_2 generation in wet grinding of granite and single-crystal powders and implications for H_2 concentration on active faults. *Geophys. Res. Lett.* **30**, 2063 (2003).
5. Saruwatari, K., Kameda, J. & Tanaka, H. Generation of hydrogen ions and hydrogen gas in quartz-water crushing experiments: an example of chemical processes in active faults. *Phys. Chem. Miner.* **31**, 176–182 (2004).
6. Li, X., Krooss, B. M., Weniger, P. & Littke, R. Liberation of molecular hydrogen (H_2) and methane (CH_4) during non-isothermal pyrolysis of shales and coals: systematics and quantification. *Int. J. Coal Geol.* **137**, 152–164 (2015).
7. Li, X., Krooss, B. M., Weniger, P. & Littke, R. Molecular hydrogen (H_2) and light hydrocarbon gases generation from marine and lacustrine source rocks during closed-system laboratory pyrolysis experiments. *J. Anal. Appl. Pyrol.* **126**, 275–287 (2017).
8. Suzuki, N., Saito, H. & Hoshino, T. Hydrogen gas of organic origin in shales and metapelites. *Int. J. Coal Geol.* **173**, 227–236 (2017).
9. Moore, G. F., Boston, B. B., Strasser, M., Underwood, M. B. & Ratliff, R. A. Evolution of tectono-sedimentary systems in the Kumano Basin, Nankai Trough fore arc. *Mar. Pet. Geol.* **67**, 604–616 (2015).
10. Kimura, G., Koge, H. & Tsuji, T. Punctuated growth of an accretionary prism and the onset of a seismogenic megathrust in the Nankai Trough. *Prog. Earth Planet. Sci.* **5**, 78 (2018).
11. Ashi, J., Tokuyama, H. & Taira, A. Distribution of methane hydrate BSRs and its implication for the prism growth in the Nankai Trough. *Mar. Geol.* **187**, 177–191 (2002).
12. Hayashi, M., Saeki, T., Inamori, T. & Noguchi, S. The distribution of BSRs related to methane hydrates, offshore Japan. *J. Jap. Assoc. Petrol. Tech.* **75**, 42–53 (2010).
13. Kida, M. et al. Chemical and crystallographic characterizations of natural gas hydrates recovered from a production test site in the eastern Nankai Trough. *Mar. Pet. Geol.* **66**, 396–403 (2015).
14. Asada, M. Definition, concept, occurrence, and recent developments in the study of mud volcanoes. *J. Geol. Soc. Japan* **126**, 3–16 (2020).
15. Fujii, T. et al. Resource assessment of methane hydrate in the eastern Nankai Trough, Japan. *Offshore Technology Conference*, Houston, Texas, USA, pp. 1-15 (2008). https://doi.org/10.4043/19310-MS.
16. Igari, S. & Sakata, S. Origin of natural gas of dissolved-in-water type in Japan inferred from chemical and isotopic compositions: Occurrence of dissolved gas of thermogenic origin. *Geochem. J.* **23**, 139–142 (1989).
17. Kato, S., Waseda, A., Nishita, H. & Iwano, H. Gas geochemistry in the Sagara district, Shizuoka Prefecture. *J. Jap. Assoc. Petrol. Tech.* **74**, 462–471 (2009).
18. Kato, S., Waseda, A. & Iwano, H. Geochemistry of natural gas and formation water from water-dissolved gas fields in Miyazaki Prefecture. *J. Jap. Assoc. Petrol. Tech.* **76**, 244–253 (2011).
19. Sakata, S., Maekawa, T., Igari, S. & Sano, Y. Geochemistry and origin of natural gases dissolved in brines from gas fields in southwest Japan. *Geofluids* **12**, 327–335 (2012).
20. Matsushita, M. et al. Regional variation of CH_4 and N_2 production processes in the deep aquifers of an accretionary prism. *Microbes Environ* **31**, 329–338 (2016).
21. Tsunogai, U. et al. Methane-rich plumes in the Suruga Trough (Japan) and their carbon isotopic characterization. *Earth Planet. Sci. Lett.* **160**, 97–105 (1998).
22. Waseda, A. & Uchida, T. The geochemical context of gas hydrate in the eastern Nankai Trough. *Resource Geol* **54**, 69–78 (2004).
23. Pape, T. et al. Hydrocarbon seepage and its sources at mud volcanoes of the Kumano forearc basin, Nankai Trough subduction zone. *Geochemistry Geophys. Geosystems* **15**, 2180–2194 (2014).

24. Ijiri, A. et al. Deep-biosphere methane production stimulated by geofluids in the Nankai accretionary complex. *Sci. Adv.* **4**, 6 (2018).
25. DeMets, C., Gordon, R. G. & Argus, D. F. Geologically current plate motions. *Geohys. J. Int.* **181**, 1–80 (2010).
26. Loveless, J. P. & Meade, B. J. Geodetic imaging of plate motions, slip rates, and partitioning of deformation in Japan. *J. Geophys. Res* **115**, B02410 (2010).
27. Argus, D. F., Gordon, R. G. & DeMets, C. Geologically current motion of 56 plates relative to the no-net-rotation reference frame. *Geochemistry, Geophys. Geosystems* **12**, Q11001 (2011).
28. Hua, Y., Zhao, D., Xu, Y. & Liu, X. Age of the subducting Philippine Sea slab and mechanism of low-frequency earthquakes. *Geophy. Res. Lett.* **45**, 2303–2310 (2018).
29. Moore, J. C., Plank, T. A., Chester, F. M., Polissar, P. J. & Savage, H. M. Sediment provenance and controls on slip propagation: lessons learned from the 2011 Tohoku and other great earthquakes of the subducting northwest Pacific plate. *Geosphere* **11**, 533–541 (2015).
30. Raimbourg, H. et al. Organic matter cracking: A source of fluid overpressure in subducting sediments. *Tectonophys* **721**, 254–274 (2017).
31. Ashi, J., Sawada, R., Omura, A. & Ikehara, K. Accumulation of an earthquake-induced extremely turbid layer in a terminal basin of the Nankai accretionary prism. *Earth Planets Space* **66**, 51 (2014).
32. Ikehara, K., Usami, K. & Kanamatsu, T. Repeated occurrence of surface-sediment remobilization along the landward slope of the Japan Trench by great earthquakes. *Earth Planets Space* **72**, 114 (2020).
33. Henry, P., Kanamatsu, T. & Moe, K. & the Expedition 333 Scientists. The Expedition 333 Scientists, Proceedings of IODP **333**: Tokyo (Integrated Ocean Drilling Program Management International, Inc.) (2012) https://doi.org/10.2204/iodp.proc.333.2012.
34. Kinoshita, M., Moore, G. F. & Kido, Y. N. Heat flow estimated from BSR and IODP borehole data: implication of recent uplift and erosion of the imbricate thrust zone in the Nankai Trough off Kumano. *Geochem. Geophys. Geosyst.* **12**, Q0AD18 (2011).
35. Harris, R. et al. A synthesis of heat flow determinations and thermal modeling along the Nankai Trough, Japan. *J. Geophys. Res. Solid Earth* **118**, 2687–2702 (2013).
36. Sugihara, T. et al. Re-evaluation of temperature at the up dip limit of locked portion of Nankai megasplay inferred from IODP Site C0002 temperature observatory. *Earth Planets Space* **66**, 107 (2014).
37. Ji, Y., Yoshioka, S. & Matsumoto, T. Three-dimensional numerical modeling of temperature and mantle flow fields associated with subduction of the Philippine Sea plate, southwest Japan. *J. Geophys. Res. Solid Earth* **121**, 4458–4482 (2016).
38. Suenaga, N. et al. Two-dimensional thermal modeling of the Philippine Sea plate subduction in central Japan: Implications for gap of low-frequency earthquakes and tectonic tremors. *J. Geophys. Res. Solid Earth* **124**, 6848–6865 (2019).
39. Screaton, E. et al. Interactions between deformation and fluids in the frontal thrust region of the NanTroSEIZE transect offshore the Kii Peninsula, Japan: Results from IODP Expedition 316 Sites C0006 and C0007. *Geochemistry Geophys. Geosystems* **10**, Q0AD01 (2009).
40. Strasser, M. et al. Origin and evolution of a splay fault in the Nankai accretionary wedge. *Nat. Geosci.* **2**, 648–652 (2009).
41. Saffer, D. M., Underwood, M. B. & McKiernan, A. W. Evaluation of factors controlling smectite transformation and fluid production in subduction zones: application to the Nankai Trough. *Island Arc* **17**, 208–230 (2008).
42. Miyakawa, A., Kinoshita, M., Hamada, Y. & Otsubo, M. Thermal maturity structures in an accretionary wedge by a numerical simulation. *Prog. Earth Planet. Sci.* **6**, 8 (2019).
43. Kimura, G. et al. Nankai forearc structural and seismogenic segmentation caused by a magmatic intrusion off the Kii Peninsula. *Geochem. Geophys. Geosyst.* **23**, e2022GC010331 (2022).
44. Burnham, A. K. Kinetic models of vitrinite, kerogen, and bitumen reflectance. *Org. Geochem.* **131**, 50–59 (2019).
45. Galimov, É. M., Prokhorov, V. S., Fedoseyev, D. V. & Varnin, V. P. Heterogenous carbon isotope effects in synthesis of diamond and graphite from gas. *Geokhimiya* **3**, 416–424 (1973).
46. Luque, F. J., Cresopo-Feo, E., Barrenechea, J. F. & Ortega, L. Carbon isotopes of graphite: implications on fluid history. *Geosci. Front.* **3**, 197–207 (2012).
47. Behar, F. et al. Experimental simulation of gas generation from coals and a marine kerogen. *Chem. Geol.* **126**, 247–260 (1995).
48. Xiong, Y. et al. The origin and evolution of thermogenic gases in organic-rich marine shales. *J. Petrol. Sci. Eng.* **143**, 8–13 (2016).
49. Waples, D. W. The kinetics of in-reservoir oil destruction and gas formation: constraints from experimental and empirical data, and from thermodynamics. *Org. Geochem.* **31**, 553–575 (2000).
50. Dalla, T., Mählmann, R. F. & Ernst, W. G. Experimental study on the pressure dependence of vitrinite reflectance. *Geochim. Cosmochim. Acta* **61**, 2921–2928 (1997).
51. Bayon, R. L., Brey, G. P., Ernst, W. G. & Mählmann, R. F. Experimental kinetic study of organic matter maturation: Time and pressure effects on vitrinite reflectance. *Org. Geochem.* **42**, 340–355 (2011).
52. Peacock, S. M. Thermal and metamorphic environment of subduction zone episodic tremor and slip. *J. Geophys. Res.* **114**, B00A07 (2009).
53. Hyndman, R. D. The seismogenic zone of subduction thrust faults: What we know and don't know. In *The seismogenic zone of subduction thrust faults* (eds. Dixon T. H. and Moore, C.) 15–40 (Columbia University Press, 2007). https://doi.org/10.7312/dixo13866-002.
54. Shi, Q. et al. Structural control and system-level behavior of the seismic cycle at the Nankai Trough. *Earth Planets Space* **72**, 27 (2020).
55. Saffer, D. M. & Tobin, H. Hydrogeology and mechanics of subduction zone forearcs: fluid flow and pore pressure. *Annual Review of Earth and Planetary Sciences* **39**, 157–186 (2011).
56. Tsang, M. et al. Hot fluids, burial metamorphism and thermal histories in the underthrust sediments at IODP 370 site C0023, Nankai Accretionary Complex. *Mar. Petrol. Geol.* **112**, 104080 (2020).
57. Kusuda, C. et al. Arima hot spring waters as a deep-seated brine from subducting slab. *Earth Planets Space* **66**, 119 (2014).
58. Kazahaya, K. et al. Spatial distribution and feature of slab-related deep-seated fluid in SW Japan. *Jour. Jap. Assoc. Hydrol. Sci* **44**, 3–16 (2014).
59. Katayama, I. Water circulation system at subduction zones. *Bull. Volc. Soc. Jpn.* **61**, 69–77 (2016).
60. Wiersberg, T., Hammerschmidt, S. B., Fuchida, S., Kopf, A. & Erzinger, J. Mantle-derived fluids in the Nankai Trough Kumano forearc basin. *Prog. Earth Planet. Sci.* **5**, 79 (2018).
61. Tomonaga, Y. et al. Fluid dynamics along the Nankai Trough: He isotopes reveal direct seafloor mantle-fluid emission in the Kumano basin (southwest Japan). *ACS Earth Space Chem* **4**, 2105–2112 (2020).
62. Price, L. C. Aqueous solubility of methane at elevated pressures and temperatures. *AAPG Bull* **63**, 1527–1533 (1979).
63. Krader, T. & Franck, E. U. The ternary systems H_2O–CH_4–NaCl and H_2O–CH_4–$CaCl_2$ to 800 K and 250 bar. *Ber. Bunsengers. Phys. Chem.* **91**, 627–634 (1987).
64. Duan, Z., Møller, N., Greenberg, J. & Weare, J. H. The prediction of methane solubility in natural waters to high ionic strength from 0 to 250 °C and from 0 to 1600 bar. *Geochim. Cosmochim. Acta* **56**, 1451–1460 (1992).
65. Duan, Z. & Mao, S. A thermodynamic model for calculating methane solubility, density and gas phase composition of methane-bearing aqueous fluids from 273 to 523 K and from 1 to 2000 bar. *Geochim. Cosmochim. Acta* **70**, 3369–3386 (2006).
66. Zhu, Z., Cao, Y., Zheng, Z. & Chen, D. An accurate model for estimating H_2 solubility in pure water and aqueous NaCl solutions. *Energies* **15**, 5021 (2022).

67. Chabab, S., Theveneau, P., Coquelet, C., Corvisier, J. & Paricaud, P. Measurements and predictive models of high-pressure H_2 solubility in brine (H_2O+NaCl) for underground hydrogen storage application. *Int. J. Hydrog. Energy* **45**, 32206–32220 (2020).
68. Scheuermann, P. P., Xing, Y., Ding, K. & Seyfried, W. E. Experimental measurement of H_2(aq) solubility in hydrothermal fluids: Application to the Piccard hydrothermal field, Mid-Cayman Rise. *Geochim. Cosmochim. Acta* **283**, 22–39 (2020).
69. Clayton, D. M. Oil and gas migration—chemical and physical constraints. *AAPG Bulletin* **63**, 761–781 (1979).
70. Shiomi, K., Takeda, T. & Ueno, T. Seismological evidence of a dehydration reaction in the subducting oceanic crust beneath western Shikoku in southwest Japan. *Geophys. J. Int* **224**, 151–168 (2020).
71. Kodaira, S. et al. A cause of rupture segmentation and synchronization in the Nankai trough revealed by seismic imaging and numerical simulation. *J. Geophys. Res.* **111**, B0901 (2006).
72. Tsuji, T., Kodaira, S., Ashi, J. & Park, J. Widely distributed thrust and strike-slip faults within subducting oceanic crust in the Nankai Trough off the Kii Peninsula. *Japan. Tectonophys.* **600**, 52–62 (2013).
73. Takasu, A. & Dallmeyer, R. D. $^{40}Ar/^{39}Ar$ mineral age constraints for the tectonothermal evolution of the Sambagawa metamorphic belt, central Shikoku, Japan: a Cretaceous accretionary prism. *Tectonophys* **185**, 111–139 (1990).
74. Wentworth, W. E., Cai, H. & Stearns, S. Pulsed discharge helium ionization detector universal detector for inorganic and organic compounds at the low picogram level. *J. Chromatogr. A* **688**, 135–152 (1994).
75. Saito, H., Suzuki, N. & Takahashi, K. Simultaneous and sensitive analysis of inorganic and organic gaseous compounds by pulsed discharge helium ionization detector (PDHID). *Geochem. J.* **46**, 255–259 (2012).
76. Martin, K. M. et al. Possible strain partitioning structure between the Kumano fore-arc basin and the slope of the Nankai Trough accretionary prism. *Geochem. Geophys. Geosyst* **11**, Q0AD02 (2010).
77. Baba, T., Tanioka, Y., Cummins, P. R. & Uhira, K. The slip distribution of the 1946 Nankai earthquake estimated from tsunami inversion using a new plate model. *Phys. Earth Planet. Inter.* **132**, 59–73 (2002).
78. Nakajima, J. & Hasegawa, A. Anomalous low-velocity zone and linear alignment of seismicity along it in the subducted Pacific slab beneath Kanto, Japan: reactivation of subducted fracture zone? *Geophys. Res. Lett.* **33**, L16309 (2006).
79. Hirose, F., Nakajima, J. & Hasegawa, A. Three-dimensional velocity structure and configuration of the Philippine Sea slab beneath Kanto district, central Japan, estimated by double-difference tomography. *J. Seism. Soc. Japan* **60**, 123–138 (2008).

Acknowledgements

We thank M. Takemura and Tokai Gas Co. for information on the occurrence of dissolved gas deposits in Yaizu and Kawane. The samples from the quasi-National Park around the Muroto Peninsula were collected in 1992 before the Muroto UNESCO Global Geopark was approved in 2011. No permissions were required for collecting the rock samples used in the present study. We thank Kochi Prefecture and Muroto City for their support in the sampling and publication of the research results. The authors are grateful to the anonymous reviewers for their valuable and constructive comments on the manuscript and suggestions for improvement of English. This research is supported by JSPS Grant-in-Aid for Scientific Research 21K03712 to NS.

Author contributions

N.S. initiated and designed the study and wrote the manuscript with input from K.K. and J.K. N.S. and K.K. contributed to the sampling and geochemical analyses. J.K. and G.K. reviewed the manuscript. All authors contributed to the discussion of the paper.

Competing interests

The authors declare no competing interests.

Additional information

Supplementary information The online version contains supplementary material available at https://doi.org/10.1038/s43247-024-01252-7.

Correspondence and requests for materials should be addressed to Noriyuki Suzuki.

Peer review information *Communications Earth & Environment* thanks Agnes Reyes and the other, anonymous, reviewer(s) for their contribution to the peer review of this work. Primary Handling Editors: Holly Stein and Joe Aslin. A peer review file is available.

Reprints and permissions information is available at http://www.nature.com/reprints

Publisher's note Springer Nature remains neutral with regard to jurisdictional claims in published maps and institutional affiliations.

Open Access This article is licensed under a Creative Commons Attribution 4.0 International License, which permits use, sharing, adaptation, distribution and reproduction in any medium or format, as long as you give appropriate credit to the original author(s) and the source, provide a link to the Creative Commons licence, and indicate if changes were made. The images or other third party material in this article are included in the article's Creative Commons licence, unless indicated otherwise in a credit line to the material. If material is not included in the article's Creative Commons licence and your intended use is not permitted by statutory regulation or exceeds the permitted use, you will need to obtain permission directly from the copyright holder. To view a copy of this licence, visit http://creativecommons.org/licenses/by/4.0/.

© The Author(s) 2024